HHS Public Access

Author manuscript

Brain Stimul. Author manuscript; available in PMC 2022 February 28.

Published in final edited form as:

Brain Stimul. 2021 ; 14(5): 1184–1196. doi:10.1016/j.brs.2021.07.009.

Evoking highly focal percepts in the fingertips through targeted stimulation of sulcal regions of the brain for sensory restoration

Santosh Chandrasekaran[a,*,#], **Stephan Bickel**[b,c,d,#], **Jose L. Herrero**[b,c], **Joo-won Kim**[e], **Noah Markowitz**[b], **Elizabeth Espinal**[b], **Nikunj A. Bhagat**[a], **Richard Ramdeo**[a], **Junqian Xu**[e], **Matthew F. Glasser**[f], **Chad E. Bouton**[a,g,**,1], **Ashesh D. Mehta**[b,c,1]

[a]Neural Bypass and Brain Computer Interface Laboratory, Feinstein Institutes for Medical Research, Northwell Health, Manhasset, NY, USA

[b]The Human Brain Mapping Laboratory, Feinstein Institutes for Medical Research, Northwell Health, Manhasset, NY, USA

[c]Department of Neurosurgery, Northwell, Manhasset, NY, USA

[d]Department of Neurology, Donald and Barbara Zucker School of Medicine at Hofstra, Northwell, Manhasset, NY, USA

[e]Departments of Radiology and Psychiatry, Baylor College of Medicine, Houston, TX, USA

[f]Departments of Radiology and Neuroscience, Washington University in St Louis, Saint Louis, MO, USA

[*]Corresponding author. schandraseka@northwell.edu, c.santosh.c@gmail.com (S. Chandrasekaran). [**]Corresponding author. Neural Bypass and Brain Computer Interface Laboratory, Feinstein Institutes for Medical Research, Northwell Health, Manhasset, NY, USA. cbouton@northwell.edu (C.E. Bouton).

[#]These authors contributed equally to this work.

[1]These authors share senior authorship.

CRediT authorship contribution statement

Santosh Chandrasekaran: Formal analysis, Writing – original draft, Writing – review & editing, performed all the experiments. analyzed data from these experiments. All authors contributed towards interpreting the results of the experiments. **Stephan Bickel:** designed the study. performed all the experiments. All authors contributed towards interpreting the results of the experiments. **Jose L. Herrero:** designed the study. All authors contributed towards interpreting the results of the experiments. **Noah Markowitz:** digitized and co-registered the electrode locations. All authors contributed towards interpreting the results of the experiments. **Elizabeth Espinal:** digitized and co-registered the electrode locations. All authors contributed towards interpreting the results of the experiments. **Nikunj A. Bhagat:** performed all the experiments, All authors contributed towards interpreting the results of the experiments. **Richard Ramdeo:** performed all the experiments. All authors contributed towards interpreting the results of the experiments. **Joo-won Kim: designed and performed the fMRI procedures at Icahn School of Medicine at Mount Sinai and analyzed the data, help using the workbench software. Junqian Xu:** designed and performed the fMRI procedures at Icahn School of Medicine at Mount Sinai and analyzed the data Software, provided key insights into cortical anatomy, help using the workbench software and generating relevant figures for the manuscript. All authors contributed towards interpreting the results of the experiments. **Matthew F. Glasser:** Software, provided key insights into cortical anatomy, help using the workbench software and generating relevant figures for the manuscript. All authors contributed towards interpreting the results of the experiments. **Chad E. Bouton:** Formal analysis, Writing – original draft, Writing – review & editing, designed the study. performed all the experiments. analyzed data from these experiments. All authors contributed towards interpreting the results of the experiments. **Ashesh D. Mehta:** designed the study. performed the SEEG leads and HD-ECoG grid implantations. All authors contributed towards interpreting the results of the experiments. All authors provided critical review, edits and approval of the final manuscript.

Declaration of competing interest

We wish to confirm that there are no known conflicts of interest associated with this publication and there has been no significant financial support for this work that could have influenced its outcome.

Appendix A. Supplementary data

Supplementary data to this article can be found online at https://doi.org/10.1016/j.brs.2021.07.009.

[g]Department of Molecular Medicine, Donald and Barbara Zucker School of Medicine at Hofstra/Northwell, Manhasset, NY, USA

Abstract

Background: Paralysis and neuropathy, affecting millions of people worldwide, can be accompanied by significant loss of somatosensation. With tactile sensation being central to achieving dexterous movement, brain-computer interface (BCI) researchers have used intracortical and cortical surface electrical stimulation to restore somatotopically-relevant sensation to the hand. However, these approaches are restricted to stimulating the gyral areas of the brain. Since representation of distal regions of the hand extends into the sulcal regions of human primary somatosensory cortex (S1), it has been challenging to evoke sensory percepts localized to the fingertips.

Objective/hypothesis: Targeted stimulation of sulcal regions of S1, using stereoelectroencephalography (SEEG) depth electrodes, can evoke focal sensory percepts in the fingertips.

Methods: Two participants with intractable epilepsy received cortical stimulation both at the gyri via high-density electrocorticography (HD-ECoG) grids and in the sulci via SEEG depth electrode leads. We characterized the evoked sensory percepts localized to the hand.

Results: We show that highly focal percepts can be evoked in the fingertips of the hand through sulcal stimulation. fMRI, myelin content, and cortical thickness maps from the Human Connectome Project elucidated specific cortical areas and sub-regions within S1 that evoked these focal percepts. Within-participant comparisons showed that percepts evoked by sulcal stimulation via SEEG electrodes were significantly more focal (80% less area; $p = 0.02$) and localized to the fingertips more often, than by gyral stimulation via HD-ECoG electrodes. Finally, sulcal locations with consistent modulation of high-frequency neural activity during mechanical tactile stimulation of the fingertips showed the same somatotopic correspondence as cortical stimulation.

Conclusions: Our findings indicate minimally invasive sulcal stimulation via SEEG electrodes could be a clinically viable approach to restoring sensation.

Keywords

Fingertip representation; Sensory percepts; Sensory restoration; Stereoelectroencephalography depth electrodes; Brain-computer interface

1. Introduction

Over 5 million people are living with paralysis in the United States alone [1] with spinal cord injury (SCI) being one of the leading causes. Up to 12% of individuals with SCI have complete tetraplegia and experience total loss of upper limb somatosensation [2]. Meanwhile, of 422 million people worldwide with diabetes mellitus [3], up to 64% can experience peripheral neuropathy leading to significant impairment of the sense of touch [4]. Such loss of sensation critically impairs the ability to perform dexterous manipulation of objects [5,6]. Intracortical brain-computer interfaces (BCI) have shown tremendous success in decoding intended movements from neural activity recorded in the primary motor cortex

[7,8] and subsequently, restoring motor control of their own hand in people with tetraplegia [9]. However, this significant progress in neurorehabilitation is often hampered by the lack of tactile feedback. Without somatosensation, users of BCI systems rely heavily on visual feedback while interacting with objects precluding fine motor control, such as manipulation of small objects, inability to detect object contact to transition from reaching to grasping, modifying grasp strength to prevent slipping, or interacting with objects outside the line of sight.

Recently, tactile percepts in the hand have been evoked in humans through intracortical microstimulation using microelectrode arrays [10–12] or cortical surface stimulation using electrocorticography (ECoG) grids [13–15] in the primary somatosensory cortex (S1), specifically cortical area 1. Although such artificial sensory feedback helps improve the user performance with a BCI system [16], focal percepts in fingertips that would be critical for dexterous manipulations as those mentioned above [17] have been difficult to achieve. In a recent study, targeting fingertip representations in the cortex required extensive intraoperative mapping using mechanical stimulation at the periphery [12] relying on spared neural pathways which may not be feasible in many patients with SCI. A primary reason for the inability to reliably evoke fingertip percepts could be that cortical stimulation in these studies has been restricted to the gyral areas of S1, i.e., the postcentral gyrus, or area 1.

Functional magnetic resonance imaging (fMRI) has shown individual digit representations to occur in the central and postcentral sulcus in addition to the postcentral gyrus, covering the cytoarchitectonically distinct cortical areas 3a, 3b, 1 and 2 [18–21]. As observed in non-human primates [22–24], these imaging studies suggest that a mirror-reversal of phalange representation occurs at the area 3b/1 border located in the central sulcus close to the crown of the postcentral gyrus. This places the proximal phalanges close to that border while more distal phalanges, including the fingertips, occur towards the area 3a/3b border located on the posterior wall of the central sulcus [18,25]. Another representation of the distal phalanges appears to occur in area 1, towards the posterior regions of the postcentral gyrus [18,25,26]. This would be consistent with the observations from a recent human somatosensory mapping study [27]. However, other studies show representation of distal phalanges closer to the 3b/1 border [28,29]. Thus, it is still unclear how the fingertip representation is distributed across the central sulcus and postcentral gyrus in human S1 [30].

Recent advances in stereotactic placement of depth electrodes, also known as stereoelectroencephalography (SEEG), increasingly provide reliable access to deeper cortical and subcortical targets in the brain [31]. These electrodes are increasingly used in the clinic for seizure onset localization in patients with medically refractory epilepsy [32]. In addition, SEEG electrodes have been used to map and document the sensory percepts evoked while stimulating the human parietal [33] and insular cortices [34]. Comparing separate cases involving SEEG and ECoG implantations, SEEG electrodes have been shown to be a clinically useful alternative for electrical brain stimulation (EBS) to map eloquent cortical areas [35,36]. In fact, a recent study showed that SEEG-mediated EBS could identify sensorimotor areas with high accuracy and specificity [37]. Moreover, implantation procedures for SEEG electrodes are minimally invasive (~2 mm craniostomy) with lower

rates of infection [38] compared to subdural strip and ECoG electrodes which require a craniotomy several centimeters wide [39].

In this first-in-human study, we explored the representation of the hand in the sulcal regions of S1 using SEEG electrodes. We implanted both SEEG and HD-ECoG electrodes in the sulcal and gyral areas of S1, respectively, in two patients with intractable epilepsy. A within-participant comparison of the percepts evoked by the two electrode types allowed us to map the hand representations in both the gyral and sulcal areas of S1 and compare the corresponding evoked percepts. Electrode implantation was guided by high-resolution fMRI obtained during a finger-tapping task analyzed using the processing pipelines of the Human Connectome Project (HCP). Upon administering intracortical direct electrical stimulation to the sulcal or gyral areas, the participants reported sensory percepts that were localized to the contralateral arm, hand, and even fingertips. Strikingly, we observed that tactile percepts evoked by sulcal stimulation were much more focused in their spatial extent. Furthermore, the percepts evoked by sulcal stimulation tended to be in and around the fingertips more often. T1-weighted (T1w) and T2-weighted (T2w) structural images provided the T1w/T2w-based myelin content and cortical thickness maps which enabled atlas-based parcellation of the cortical areas, somatotopic subregions, and sub-areas of the sensorimotor cortex [40] further informing location of electrodes and the corresponding evoked percepts. SEEG-mediated recording of neural activity in the sulcal areas evoked upon mechanical tactile stimulation enabled precise localization of cortical regions involved in processing of sensory information from specific finger and palm regions.

These results demonstrate that stimulation of sulcal regions of S1 can be achieved using SEEG and can activate fingertip representations. Combined with the minimally invasive implantation procedure for SEEG electrodes, this approach for sulcal stimulation can be an effective and reliable for evoking focal percepts in the hand and fingers that are functionally relevant to people with tetraplegia. Furthermore, they can be an effective tool for passive mapping of the brain for clinical purposes.

2. Methods

Participants:

Two patients undergoing pre-operative seizure monitoring for surgical treatment of intractable epilepsy took part in this study. Participant 1 was implanted with SEEG leads for 7 days after which they were explanted. Mapping of percepts evoked by stimulating through these electrodes was performed on Day 6 post-implant. About 3 months later, the patient was implanted with HD-ECoG grids for 8 days and percept mapping was performed on day 7 post-implant. In case of participant 2, SEEG leads were implanted for 14 days. About a month later, the participant was implanted with HD-ECoG grids for 10 days. Recording of neural activity with SEEG electrodes in response to peripheral tactile stimulation was done on Day 9 post-implant. Percept mapping was performed on Day 12 and Day 9 for SEEG and HD-ECoG electrodes, respectively. Recording of neural activity using SEEG electrodes helped localize the seizure onset close to the sensorimotor areas. However, additional grid electrodes were needed to further localize the seizure onset and, more importantly, the borders of sensorimotor cortices to help guide the resection. This two-staged approach of

implanting SEEG leads followed by grid and/or strip electrodes is often used in such a situation at the Comprehensive Epilepsy Center at Northwell Health.

The decisions regarding whether to implant, the electrode targets, and the duration for implantation were based entirely on clinical grounds without reference to this investigation. Based on these clinical indications, all electrodes were implanted in the right hemisphere for both participants. Patients were informed that participation in this study would not alter their clinical treatment, and that they could withdraw from the study at any time without jeopardizing their clinical care. All procedures and experiments were approved by the Northwell Institutional Review Board and participants provided informed consent prior to enrollment into the study.

Imaging:

Participants were scanned a week before their first implant on a 3T MRI scanner (Skyra, Siemens, Germany) with a 32-channel head coil. HCP-like structural and functional MRI were acquired: T1-weighted (T1w) 3D MPRAGE sequence, 0.8 mm isotropic resolution, TR/TE/TI = 2400/July 2, 1000 ms, flip angle = 8°, in-plane under-sampling (GRAPPA) = 2, acquisition time 7 min; T2-weighted (T2w) 3D turbo spin echo (SPACE) sequence, 0.8 mm isotropic resolution, in-plane under-sampling (GRAPPA) = 2, TR/TE = 3200/564 ms, acquisition time 6.75 min; task fMRI using the CMRR implementation of multiband gradient echo echo-planar imaging (EPI) sequence [41], 2.1 mm isotropic resolution, 70 slices with a multiband factor of 7 [42], FOV 228 mm × 228 mm, matrix size 108 × 108, phase partial Fourier 7/ 8, TR/TE = 1000/35 ms, flip angle = 60°, phase encoding direction = anterior-posterior (A-P), echo spacing = 0.68 ms, 240 vol in 4 min; and a pair of reversed polarity (A-P/P-A) spin echo EPI field mapping acquisitions with matched echo train length and echo spacing to the fMRI acquisition. The task was button-pressing on the PST button response unit (Psychology Software Tools, Sharpsburg, PA, USA) using a single finger (wrist restrained with strap on the button response unit and neighboring fingers taped down with medical tape), repeating 6 times of 20-s off (resting with cue of a blank dark screen) and 20-s on (tapping with continuous video cue of the same finger motion presented from a projector screen). Participant 1 performed task once for each of thumb, index, and little fingers (phase-encoding direction A- > P) while participant 2 performed two repetitions for each of thumb, index, and middle fingers (phase-encoding directions A- > P and P- > A). Due to limited scanner time, we consistently used three fingers in the button task. The motivation for including digits 1, 2, and 5 in participant 1 was to map the extents of the hand while in participant 2, our motivation evolved to focus on the first three digits as they are functionally more important in grasping and manipulating objects. The MRI preprocessing began with the HCP minimal preprocessing pipelines version 3.27 [43] including, motion correction, distortion correction, cortical surface reconstruction and subcortical segmentation, generation of T1w/T2w-based myelin content and cortical thickness maps, transformation of the fMRI data to MNI and CIFTI grayordinate standard spaces using folding-based registration with MSMSulc [44,45], and 2 mm FWHM surface and subcortical parcel constrained smoothing for regularization. The fMRI data were cleaned of spatially specific structured noise using the HCP's multi-run (version 4.0) ICA-FIX [46e48] for multi fMRI (multiple finger tasks) and linear trends without regressing

out motion parameters. Somatotopic functional responses were estimated (first-level for participant 1 and second-level fixed-effect averaging of the two phase-encoding directions for participant 2) using a generalized linear model (GLM)-based fMRI analysis [49]on the grayordinate data space for each finger.

Electrode localization:

The SEEG electrodes (Model Number 2102–16-093, PMT Corporation, Chanhassen, MN, USA) consisted of 16 contacts, cylinders with 2 mm length, 0.8 mm diameter, and 4.43 mm spacing (center to center) with about 5.02 mm^2 of surface area per contact. The lead spanned a length of 68.5 mm from tip to end of last contact. The HD-ECoG grids (PMT Corporation) consisted of 2 mm diameter flat contacts with 3.14 mm^2 surface area per contact, in an 8 × 8 arrangement with 5 mm spacing (center to center) in participant 1 with and a 16 × 16 contact arrangement with 4 mm spacing in participant 2. Since both patients had clinical indications that required mapping of the sensorimotor cortex, task-based fMRI activation maps were used to guide electrode placement.

For digital localization of the electrodes, we used the freely available iElvis toolbox, available at https://github.com/iELVis/ [50]. Briefly, the electrodes were manually localized using the software BioImage Suite (http://www.bioimagesuite.org) on a postimplant CT which was co-registered using an affine transformation (6 degrees-of-freedom FLIRT; www.fmrib.ox.ac.uk/fsl) to a preimplantation 3T high-resolution T1w MRI. We used the Free-Surfer [51] output from the HCP minimal processing pipeline [40] to obtain the pial surface. The subdural HD-ECoG electrodes were projected to the smoothed pial surface. The smoothed pial surface, also called the outer smoothed surface, is generated by Freesurfer and wraps tightly around the gyral surfaces of the pial layer while bridging over the sulci. No correction was applied to SEEG electrode coordinates.

To visualize the fMRI activation maps and the electrodes simultaneously, we used HCP Connectome Workbench. Before importing the electrode coordinates into Workbench, we applied a RAS coordinate offset (the right-hand coordinate system of R = thumb, A = index, and S = middle finger) as follows – *transformed_RAS_coordinates* = *Norig*inv(Torig)*RAS_coordinates* where the transformation matrices *Norig* is obtained by *mri_info –vox2ras [subject]/mri/orig.mgz* and *Torig* is obtained by *mri_info –vox2ras-tkr [subject]/mri/orig.mgz*.

The transformed coordinates were then imported as foci using the T1w surfaces into a developmental version of Connectome Workbench.

Electrical brain stimulation (EBS):

Intracranial EBS is a routine clinical procedure to identify eloquent cortex to be spared from surgical resection. Generally, EBS was carried out towards the end of implantation period after sufficient seizure data had been collected and participants were back on their anti-seizure medications.

For this study, we used routine EBS parameters with a S12D Grass current-controlled cortical stimulator (Grass Technologies, Pleasanton, CA). We used pairs of electrodes for

bipolar stimulation and delivered current-regulated, symmetric biphasic square-wave pulses with 0.2 ms width per phase, at 20 or 50 Hz, with stimulation amplitudes between 0.5 and 6 mA, for 0.5–2 s while the participant was quietly resting and asked to report the occurrence of any sensation. The different sites were first screened for a possible percept with 50 Hz stimulation - a stimulation frequency that provides a good trade-off between obtaining a stimulation effect and eliciting a seizure and is in accordance with common procedure established across up to 70% of epilepsy monitoring centers [52]. The stimulation amplitude was initially set at 0.5 mA the lowest possible amplitude on the clinical stimulator. If no percept was evoked, the stimulation amplitude was increased in gross (~0.5 mA) increments until a percept was elicited, or after-discharges occurred, up to a maximal amplitude of 6 mA. Once a percept was felt the amplitude was more finely adjusted (using the analogue adjustment knob) to find the threshold of perception. The stimulation was repeated at this final threshold value at least two times to ensure the evoked percept was consistent. If a percept was evoked even at 0.5 mA at 50 Hz, the frequency was decreased to the next frequency (20 Hz) and the above process was repeated. The stimulation pulse had a cathodic leading phase. Stimulation time was always limited to a maximum of 2 s. Stimulation was stopped immediately and much before the maximum time had elapsed if the subject reported a sensation. For every sensation on the hand that was reported, the participant was asked to draw the affected area on a schematic of a hand. The sensations were described as “tingling” or “sensation of electricity”. While the intensity of the percepts changed with stimulation amplitude, none of the other qualities of the evoked percepts such as location, size, and qualitative description changed with stimulation amplitude.

Without informing the participant, sham trials (0 mA stimulation) were intermixed with real stimulation trials to rule out any placebo effects. Intracranial EEG was acquired continuously using a clinical recording system (XLTEK, Natus Medical) at 512 Hz or 1 kHz and monitored across all implanted electrodes for the presence of after-discharges and seizures. No seizures were caused during stimulation of the areas reported here.

Analysis of sensory percepts:

For this study, we focused our analysis to the sensory percepts localized to the hand and wrist. Some of the SEEG and HD-ECoG electrodes did evoke complex percepts that included both sensory as well as motor components, including percepts that were accompanied with an overt movement or a sensation of movement, presumably a proprioceptive sensation. We included only those electrodes that evoked a tactile sensation by itself, without any overt or perceived sensation of movement. To digitize the participant responses, we used a script custom-written in MATLAB to redraw the participant drawings on a computer. Surface areas of the digitized percepts were then calculated and used for all further analysis.

Recording of neural activity:

In addition to the clinical recording system, neural activity was recorded for participant 2 using SEEG electrodes with a Neuroport System (Blackrock Microsystems, Salt Lake, Utah) with a sampling rate of 10 kHz while performing mechanical stimulation of the fingertips of their left hand. We used a Semmes-Weinstein Monofilament (TouchTest Sensory Probes)

of evaluator size, 4.31 (2 g). A visual cue, visible only to the experimenter and not the participant, signaled the start and end of each repetition as well as the specific finger to which the mechanical stimuli was to be targeted. During this period, the experimenter repeatedly tapped the cued finger with a Semmes-Weinstein Monofilament repeatedly, approximately once every second. This cue signal was aligned to the recorded neural data to analyze only the epochs of stimuli. Due to time constraints and patient fatigue, we unfortunately were not able to perform the recording task in participant 1.

Two separate electrodes located in soft tissue lacking neural activity were used for the system ground and for the reference. Subsequent analysis involved multiple steps to extract information regarding power modulation in different frequency bands. Signals from neighboring electrodes were subtracted in software to provide bipolar data with reduced noise. Non-overlapping Blackman windows of 200 ms in length were applied, followed by a short Fast Fourier Transform (sFFT) for each window (with a resulting frequency resolution of 5 Hz). The signal amplitudes at each frequency were then integrated (averaged) across pre-selected frequency bands as follows: 0–10, 10–15, 15–30, 30–100, 100–500, and 500–5000 Hz. These frequency bands have been shown to contain signals with amplitude modulation with a high degree of repeatability (high temporal correlation) related to movement and tactile stimuli [53]. These amplitude features for all bipolar recordings were standardized by subtracting their mean and dividing by their standard deviation across the entire task. For the analysis in this study, we chose neural activity in the high gamma or 100–500 Hz frequency band. Numerous invasive studies have shown that high-gamma power changes in the sensorimotor area are associated with passive somatosensory stimulation [54–56]. Epochs aligned with each visual cue (animated hand) presented to the participant during each task were created, starting at the cue onset, and extending to 400 ms after the cue offset. All aligned trials for each epoch (cue) type were averaged to form a composite temporal response. To quantify the degree of repeatability, or temporal correlation, the mean correlation coefficient (MCC) was computed by averaging the correlation coefficients obtained for the amplitude features for each trial with respect to their cue-aligned composite [53].

3. Results

Study participants were first implanted with SEEG leads, subsequently replaced by a HD-ECoG grid, for extraoperative monitoring of neural activity to localize the epileptogenic zone. During routine clinical intracranial EBS using either of these electrodes, participants were asked to report the sensory percepts that were evoked. A total of 28 SEEG electrode contacts each were localized to S1 and the nearby white matter in the two participants. For HD-ECoG, participant 1 had 22 contacts over S1 while participant 2 had 57 contacts over S1 (Table 1). For this study, we focused on the sensory percepts localized to the hand and wrist. Stimulation amplitudes that evoked sensations in the hand area ranged from 0.5 to 6 mA with stimulation frequencies of either 20 or 50 Hz, and a pulse width of 200 μs. After each stimulation trial (lasting 0.5–2 s), the evoked percept was reported by the participant and was recorded by the experimenter. A total of 40 electrode pairs (5 & 6 SEEG electrode pairs, and 10 & 19 HD-ECoG electrode pairs in participants 1 and 2, respectively) across the two participants evoked at least one sensory percept in the contralateral hand or arm.

Other electrodes evoked percepts that were localized to more proximal areas of the arm or even perceived bilaterally. These were not included for analysis in this study. The mean stimulus amplitude for SEEG-mediated sulcal stimulation at threshold of perception was 1.09 ± 1.07 mA and 1.59 ± 1.68 mA for participants 1 and 2, respectively given stimulation frequency of predominantly 20 Hz. Meanwhile, mean stimulus amplitude at threshold for gyral stimulation with HD-ECoG electrodes was 0.989 ± 0.37 mA and 2.25 ± 1.23 mA for participants 1 and 2, respectively with a stimulation frequency of 50 Hz. It is worth noting that the stimulation frequency had to be lowered to 20 Hz to determine the thresholds for SEEG electrodes as compared to HD-ECoG electrodes (50 Hz). Since the lowest stimulation amplitude possible was restricted to 0.5 mA, the threshold search procedure included the drop down in frequency to allow more granularity in threshold determination as described in the Methods. All stimulation amplitude, frequencies and percept descriptions at threshold are included in Tables 2 and 3.

3.1. HD-ECoG and SEEG electrodes provide access to different cortical areas

To locate the representation of the fingers in S1 (Fig. 1 insets), the participants performed button-press tasks using thumb (D1, red), index (D2, green), and little finger (D5, blue, participant 1) or middle finger (D3, blue, participant 2) during functional imaging. The motivation for including digits 1, 2, and 5 in participant 1 was to map the extents of the hand while in participant 2, our motivation evolved to focus on the first three digits, as they are functionally more important in grasping and manipulating objects. The fMRI activation results were thresholded to optimize the visualization of topological features in area 3b (Fig. 1, right panels), located on the posterior wall of the central sulcus, and overlaid (from top to bottom without transparency: red, green, and blue) on group average cortical areal maps [40]. Fig. S1 demonstrates that the group average cortical areal definitions align well with the individual subject cortical myelin and thickness maps. Overlapping activation in area 4 (anterior wall of the central sulcus) and 3a (fundus of the central sulcus) are evident (most of the blue and a large portion of the green are hidden beneath the red color) in both participants. A topologically meaningful representation of D1, D2, and D3/D5 can be observed in the lateral-medial axis in area 3b in both participants. Interestingly, activation in regions medial to the D3/D5 representation can be observed in D1 (red) and D2 (green) tasks. Less consistent individual digit representations were observed in area 1 (postcentral gyrus), except for an overlapping activation in the lateral location of D1 for all finger tasks. Even less consistent or appreciable activations exist in area 2 at the chosen threshold level (Fig. S2).

We were interested in further elucidating the digit representations in the sulcal and gyral areas of S1. Specifically, we wanted to determine whether electrical stimulation using SEEG depth electrodes can effectively target these digit representations in the sulcal areas of S1. Overlaying the electrodes that evoked sensations in the hand on top of the fMRI maps shows that the HD-ECoG electrodes (fuschia spheres in Fig. 1) appear to cluster in area 1 which covers the apical surface of the postcentral gyrus. Meanwhile, the SEEG electrodes (cyan spheres in Fig. 1) that evoked sensory percepts in the hand, when projected to the cortical surface, localize predominantly to the areas 3a and 3b of S1 which are located at the fundus and posterior wall of the central sulcus, respectively. In case of SEEG, the

electrode pairs always consisted of adjacent electrodes within the same lead. The orientation of all HD-ECoG electrode pairs was parallel to the example electrode pair shown for each participant in Fig. 1 (white rectangle).

3.2. Fingertip percepts evoked by sulcal stimulation

We characterized the sensory percepts evoked by direct electrical stimulation of S1 gyral and sulcal areas using HD-ECoG or SEEG electrodes, respectively. In both participants, electrical stimulation was gradually ramped up until percept threshold was reached, at which point the participants described what they perceived. We observed that the percepts evoked by sulcal stimulation tended to be highly focal, often restricted to within a single segment of a finger, and often at the fingertips. The SEEG electrodes that evoke these percepts were predominantly located near the anterior wall of the postcentral gyrus (Fig. 2, panels A and C; Fig. S3). Meanwhile, the percepts evoked by gyral stimulation often extended over multiple segments of a digit or multiple digits (Fig. 2, panels B and D). Interestingly, we observed a paucity in percepts restricted to fingertips alone when stimulating S1 gyral areas. As expected, the evoked percepts exhibit a somatotopical organization of the hand, with thumb percepts evoked by electrodes that were more laterally located, while percepts in the index and middle fingers and the wrist were evoked by electrodes that were more dorsal (Fig. 2D).

3.3. Focal and distal percepts evoked by sulcal stimulation

Comparing the areas enclosed by the sensory percepts showed that sulcal stimulation using SEEG electrodes evoked percepts that were significantly smaller than those evoked by gyral stimulation using HD-ECoG electrodes (Fig. 3A, $p = 0.02$, Wilcoxon ranksum test, $\chi^2 = 5.57$). This suggests that the sensory percepts evoked by sulcal stimulation tend to be more focal in their spatial spread. Comparing the probability of occurrence of percepts of different sizes also showed significant skew towards percepts with smaller area in case of sulcal stimulation (Fig. 3B, $p \ll 0.01$, Kolmogorov-Smirnov test).

To evaluate if there was a difference in the location of the percepts evoked by gyral and sulcal stimulation, we determined the probability that an evoked percept covered a particular area of the hand. Fig. 4 shows a probability of a percept covering a region of the hand normalized to the maximal number of percepts covering any area of the hand. Fingertips are most often covered by percepts evoked by SEEG-mediated sulcal stimulation (Fig. 4A) while gyral stimulation evoked percepts cover the middle phalanges most often (Fig. 4B). Percepts covering the index fingertip sensation were evoked most often (evoked by 4 electrodes) followed by middle and ring fingertips (evoked by 3 electrodes). Given that 12 SEEG electrodes evoked sensations localized to the hand and wrist, percepts that spread over the fingertips constituted up to 2530% of those evoked by SEEG electrodes located in the sulcal regions of S1. In comparison, only 6–12% of the percepts evoked by the electrodes locate on the postcentral gyrus (2–4 out of 31 electrodes) covered the fingertips while the most represented region of the hand were the middle phalanges of the fingers and the ulnar side of the hand (up to 30%).

3.4. Cortical activity recorded during mechanical tactile stimuli

While implanted with SEEG electrodes, participant 2 also received mechanical tactile stimulation of the thumb, index and middle finger pads and the resultant neural activity in S1 was recorded (see Fig. S4). We aimed to further confirm the previously identified sulcal locations were involved in fingertip tactile sensation. We identified electrodes from which neural activity were recorded that showed a high degree of repeatability (mean correlation coefficient, $r \geq 0.6$) among features in the high gamma band (100–500 Hz) across repeated cycles of mechanical stimulation, i.e., tapping of the fingertips. We show that sulcal electrodes recording stimulus evoked somatosensory activity were spatially clustered (Fig. 5A). Interestingly, the sulcal electrodes that evoked a sensory percept in the hand overlapped or were located close to the sulcal electrodes that were activated by tactile stimulation of the fingertips (Fig. 5B).

4. Discussion

In this study, we demonstrate that sulcal stimulation in human S1 evokes sensory percepts localized to the fingertips more often than gyral stimulation. SEEG electrodes provided an effective way to deliver targeted electrical stimulation to sulcal regions of S1. Using these electrodes, in two participants, we were able to evoke sensory percepts restricted to single segments of a digit, including fingertips and more focal than those evoked by gyral stimulation using HD-ECoG electrodes. We were also able to record neural correlates of mechanical tactile stimuli delivered at the fingertips on sulcal contacts that were spatially clustered. The findings in this study suggest that evoking fingertip percepts through intracortical stimulation would require accessing the sulcal regions of S1. Additionally, it shows the potential of electrodes targeted to the sulcal regions in providing intuitive and useful somatosensory feedback for dexterous hand movements in sensorimotor BCIs.

We used neuroimaging tools designed by the Human Connectome Project to elucidate the precise subregions of S1 in relation to electrode implantation. Though the fMRI activation maps highlight the somatotopic subregion corresponding to the hand area in S1, the cortical areas of S1 are not clearly delineated. In this study, the intrinsic blood-oxygen-level-dependent (BOLD) point spread function at 3T, and the less well-defined finger task do not allow us to detect fMRI activation patterns of the distal (i.e., fingertip) vs proximal phalanges. However, previous studies with 7T fMRI have been able to localize representation of the fingertips in S1 [18]. The group average cortical parcellations based on T1w/T2w-based myelin content and cortical thickness maps could effectively guide implantation of SEEG electrodes to target the finger representations in S1.

The well-known somatotopy of the human S1 represents the digits D1 (thumb) to D5 (little finger) in lateral-to-medial succession from the lateral border of the upper extremity subregion. Such somatotopic mapping was characteristically depicted in the task fMRI activations in area 3b in both participants [20,21], notwithstanding the possibility of visually-driven contribution [57], while thenar (muscles under the base of the thumb) and palm sensation during finger tapping likely account for the activations observed in areas medial to the D5 representation. We interpret the overlapping activations from all fingers within the representation of D1 in area 1 as an inadvertent result of increased

counter-balance pressure of the thumb pressing against the surface underneath, while the other fingers were lifted during finger tapping. Among the fingers, the thumb shows the most consistent and distinct representation in the expected somatotopic subregion. This is consistent with the relatively isolated anatomical structure of D1 from other fingers. The less consistent and focal representation of the other fingers are potentially due to a couple of reasons. First, unlike other elegant sensory task designs with dedicated tactile or electrical stimulation devices for each finger, sensory activations from common motor tasks are inherently imprecise despite best-efforts in task instruction and subject compliance. Second, the isolation of single digit motion is much more difficult for the rest of the digits than the thumb.

Our observation of sulcal stimulation in human S1 evoking fingertip percepts more often than gyral stimulation is in agreement with functional imaging studies that have predominantly localized fingertip representation to the posterior wall of the central sulcus (area 3b) and occasionally at the crown of the postcentral gyrus [18–21,28]. With the mirror-reversal of representation occurring at the area 3b-1 border, the representation of fingertips might still extend into the posterior regions of the postcentral gyrus as shown by some imaging [25,26,30] and recent stimulation studies [27]. However, in our study, we had only two SEEG contacts located deep in the postcentral sulcus in one participant that evoked percepts in the hand. None of the electrodes located in the posterior regions of the postcentral gyrus evoked fingertip percepts. It might be the case that the fingertip representations on the crown of the postcentral gyrus are small and require extremely precise targeting, while they are more extensive within the central sulcus and hence, easily accessible with SEEG electrodes.

Recently, both microelectrode arrays and ECoG grid electrodes have been used to provide artificial sensory feedback. While individual microelectrode array contacts evoke highly focal percepts restricted to individual phalanges, by activating very closely spaced cortical locations they provide only limited coverage of the hand, often restricted to only a few phalanges over two or three fingers [10–12]. Such high degree of anatomical overlap among the evoked percepts restricts the amount of sensory information that can be conveyed. Meanwhile, with larger size and inter-contact spacing when compared to microelectrode arrays, HD-ECoG electrodes elicit sensory percepts that tend to cover either multiple phalanges or entire digits [13,15,58]. Additionally, with the capability to record or modulate the neural activity of neurons that lie within 1–2mm below the cortical surface [59], these electrodes provide access to only the gyral surfaces of the cortex.

With the potential to reach sulcal areas of the cortex, SEEG electrodes provide a unique advantage of being able to evoke tactile sensations that are perceived to emanate from the fingers, particularly fingertips. A recent study has reported being able to target fingertip representations on the postcentral gyrus using microelectrode arrays in a patient with SCI [12]. However, such precise targeting was possible only after performing extensive intraoperative mapping of neural responses in S1 to peripheral stimulation of the fingertips relying on the relatively intact residual sensory pathways. Such an approach based on evoked responses in S1 might not be feasible in case of other potential users of BCI with more severe loss of function. It is well established that motor imagery can be used to

identify the hand area of the motor cortex in people with tetraplegia [9]. Moreover, in able-bodied individuals, motor imagery has been shown to activate both primary motor and somatosensory cortices [60]. In addition, the finger regions of the primary motor cortex and somatosensory cortex are juxtaposed against each other across the central sulcus [61]. We therefore expect that motor imagery alone can help localize the finger regions in the somatosensory cortex in people with high-level tetraplegia guiding minimally invasive SEEG implantation.

SEEG electrodes have recently been gaining favor for seizure onset localization as well as for mapping eloquent areas of the cortex in case of medically refractory epilepsy [32]. In contrast to other intracranial electrodes that require burr holes or large craniotomies for implantation, SEEG electrodes can be implanted using a minimally invasive approach via a 1–2 mm craniostomy [31]. The minimally invasive approach for their implantation reduces the risk of hemorrhage and infection to 1% and 0.8% respectively from that of 4% and 2.3% for subdural electrodes such as ECoG grids [38,39].

In this study, all stimulation was done using a bipolar configuration involving adjacent electrodes. While the inter-contact spacing are comparable (4–5 mm in HD-ECoG vs 4.43 mm in SEEG) between the two electrode types, the surface area of SEEG electrodes (~5 mm^2) are almost twice that of HD-ECoG electrodes (~3 mm^2). Combined with the lack of directionality, SEEG electrodes should potentially activate a wider area of cortex evoking bigger or mixed percepts. The high-level of two-point discrimination at fingertips is due to the high density of mechanoreceptors as well as smaller receptive fields for fingertips in S1. Stimulating cortical areas with small receptive fields have been shown to evoke smaller percepts in the human visual cortex [62]. A similar relationship between receptive field and percept size in S1 would enable cortical stimulation targeted at fingertip representations to evoke smaller percepts. It is possible that the difference in receptive field sizes between gyral and sulcal areas are a stronger determining factor of the evoked percept size than the electrode form factor.

Future studies should explore denser, smaller and even directional SEEG electrodes that could restrict the effective volume of cortical tissue that is activated and thus, evoke more focal percepts. However, higher current density and the potential tissue damage are factors that will have to be considered as well. Another potential limitation of the current study is the low number of participants. However, we specifically included only those participants who had at least 2 or more electrodes in S1 that evoked percepts in the hand area. Moreover, the two participants included were implanted with both types of electrodes enabling a within-patient comparison. Proprioception is potentially as critical as tactile percepts for dexterous motor control. We did not explicitly explore evoking proprioceptive percepts in this study. Non-human primate studies have shown that area 3a, located at the fundus of the central sulcus, has the largest incidence of proprioceptive cells [63]. SEEG electrodes present one of the best avenues to explore the effectiveness of evoking proprioceptive percepts by stimulating area 3a.

The MCC (repeatability metric) of recorded neural activity during mechanical tactile stimulation of the fingertips highlighted SEEG contacts that were either identical or

adjacent to those that evoked percepts in the hand. This overlap between receptive fields of mechanical stimuli at the periphery and the percept field evoked by cortical stimulation was potentially due to the relatively large size of the electrodes resulting in both activation as well as recording of neural activity of a relatively large pool of local neurons as compared to microelectrode arrays. This further supports that the sulcal locations identified during electrical stimulation are indeed related to and important in tactile sensory restoration. This could also potentially provide a safer way to map eloquent cortex avoiding direct electrical stimulation which could trigger after-discharges or seizure activity [64] as well as for recording task-related, highly relevant neural activity for BCI applications.

Thus, we have shown that the representation of fingertips is readily accessible on the posterior wall of the central sulcus using SEEG electrodes. This suggests that sulcal stimulation mediated by SEEG electrodes offer a highly viable alternative to the current approaches restricted to gyral stimulation for restoring somatosensation. Future technical developments that will allow tightly spaced electrodes are important for greater success and efficacy. A recent review explored the potential of SEEG electrodes in BCI applications for decoding intended movement [65]. Combined with our findings on sulcal stimulation being able to provide highly focal and relevant somatosensory feedback, we venture that SEEG electrodes can potentially become an established approach for sensorimotor restoration in closed loop BCI applications. Moreover, with the ability of reaching deeper structures of the cortex, SEEG-mediated stimulation can potentially mitigate sensorimotor deficits arising due to even subcortical strokes along the cortico-spinal tract.

Supplementary Material

Refer to Web version on PubMed Central for supplementary material.

Acknowledgements

We would like to thank our participants for their extraordinary commitment to this study, their patience with the experiments, and the deep insights provided by them, the clinicians and researchers at Feinstein Institutes for Medical Research. We would also like to thank Kevin Tracey, MD for providing critical inputs on the manuscript.

Funding

This study was funded through support provided by Feinstein Institutes for Medical Research at Northwell Health and partly funded by Empire Clinical Research Investigator Program (ECRIP) Fellowship of which SB was a recipient. MFG was supported by NIH R01MH060974.

References

[1]. Armour BS, Courtney-Long EA, Fox MH, Fredine H, Cahill A. Prevalence and causes of paralysis-United States, 2013. Am J Publ Health 2016;106:1855–7. 10.2105/AJPH.2016.303270.

[2]. NSCISC. Facts and figures at a glance. 2020.

[3]. Zhou B, Lu Y, Hajifathalian K, Bentham J, Di Cesare M, Danaei G, et al. Worldwide trends in diabetes since 1980: a pooled analysis of 751 population-based studies with 4$4 million participants. Lancet 2016;387: 1513–30. 10.1016/S0140-6736(16)00618-8. [PubMed: 27061677]

[4]. Ennis SL, Galea MP, O'Neal DN, Dodson MJ. Peripheral neuropathy in the hands of people with diabetes mellitus. Diabetes Res Clin Pract 2016;119: 23–31. 10.1016/j.diabres.2016.06.010. [PubMed: 27420380]

[5]. Rothwell JC, Traub MM, Day BL, Obeso JA, Thomas PK, Marsden CD. Manual motor performance in a deafferented man. Brain 1982;105:515–42. 10.1093/brain/105.3.515. [PubMed: 6286035]

[6]. Monzée J, Lamarre Y, Smith AM. The effects of digital anesthesia on force control using a precision grip. J Neurophysiol 2003;89:672–83. 10.1152/jn.00434.2001. [PubMed: 12574445]

[7]. Hochberg LR, Bacher D, Jarosiewicz B, Masse NY, Simeral JD, Vogel J, et al. Reach and grasp by people with tetraplegia using a neurally controlled robotic arm. Nature 2012;485:372–5. 10.1038/nature11076. [PubMed: 22596161]

[8]. Collinger JL, Wodlinger B, Downey JE, Wang W, Tyler-Kabara EC, Weber DJ, et al. High-performance neuroprosthetic control by an individual with tetraplegia. Lancet 2013;381:557–64. 10.1016/S0140-6736(12)61816-9. [PubMed: 23253623]

[9]. Bouton CE, Shaikhouni A, Annetta NV, Bockbrader MA, Friedenberg DA, Nielson DM, et al. Restoring cortical control of functional movement in a human with quadriplegia. Nature 2016;533:247–50. 10.1038/nature17435. [PubMed: 27074513]

[10]. Flesher SN, Collinger JL, Foldes ST, Weiss JM, Downey JE, Tyler-Kabara EC, et al. Intracortical microstimulation of human somatosensory cortex. Sci Transl Med 2016;8:361ra141. 10.1126/scitranslmed.aaf8083.

[11]. Armenta Salas M, Bashford L, Kellis S, Jafari M, Jo H, Kramer D, et al. Proprioceptive and cutaneous sensations in humans elicited by intracortical microstimulation. ELife 2018;7:e32904. 10.7554/eLife.32904. [PubMed: 29633714]

[12]. Fifer MS, McMullen DP, Thomas TM, Osborn LE, Nickl RW, Candrea DN, et al. Intracortical microstimulation elicits human fingertip sensations. MedRxiv 2020. 10.1101/2020.05.29.20117374. 2020.05.29.20117374.

[13]. Hiremath SV, Tyler-Kabara EC, Wheeler JJ, Moran DW, Gaunt RA, Collinger JL, et al. Human perception of electrical stimulation on the surface of somatosensory cortex. PloS One 2017;12:e0176020. 10.1371/journal.pone.0176020. [PubMed: 28489913]

[14]. Lee B, Kramer D, Armenta Salas M, Kellis S, Brown D, Dobreva T, et al. Engineering artificial somatosensation through cortical stimulation in humans. Front Syst Neurosci 2018;12:24. 10.3389/fnsys.2018.00024. [PubMed: 29915532]

[15]. Kramer DR, Lee MB, Barbaro M, Gogia AS, Peng T, Liu C, et al. Mapping of primary somatosensory cortex of the hand area using a high-density electrocorticography grid for closed-loop brain computer interface. J Neural Eng 2020. 10.1088/1741-2552/ab7c8e.

[16]. Flesher SN, Downey JE, Weiss JM, Hughes CL, Herrera AJ, Tyler-Kabara EC, et al. A brain-computer interface that evokes tactile sensations improves robotic arm control. Science 2021;372(6544):831–6. 10.1126/science.abd0380. [PubMed: 34016775]

[17]. Johansson RS, Flanagan JR. Coding and use of tactile signals from the fingertips in object manipulation tasks. Nat Rev Neurosci 2009;10:345–59. 10.1038/nrn2621. [PubMed: 19352402]

[18]. Sanchez-Panchuelo RM, Besle J, Beckett A, Bowtell R, Schluppeck D, Francis S. Within-digit functional parcellation of brodmann areas of the human primary somatosensory cortex using functional magnetic resonance imaging at 7 tesla. J Neurosci 2012;32:15815–22. 10.1523/JNEUROSCI.2501-12.2012. [PubMed: 23136420]

[19]. Martuzzi R, van der Zwaag W, Farthouat J, Gruetter R, Blanke O. Human finger somatotopy in areas 3b, 1, and 2: a 7T fMRI study using a natural stimulus. Hum Brain Mapp 2014;35:213–26. 10.1002/hbm.22172. [PubMed: 22965769]

[20]. Kolasinski J, Makin TR, Jbabdi S, Clare S, Stagg CJ, Johansen-Berg H. Investigating the stability of fine-grain digit somatotopy in individual human participants. JNeurosci2016;36:1113–27.10.1523/JNEUROSCI.1742-15.2016. [PubMed: 26818501]

[21]. Sanchez Panchuelo RM, Ackerley R, Glover PM, Bowtell RW, Wessberg J, Francis ST, et al. Mapping quantal touch using 7 Tesla functional magnetic resonance imaging and single-unit intraneural microstimulation. ELife 2016;5:e12812. 10.7554/eLife.12812. [PubMed: 27154626]

[22]. Merzenich MM, Kaas JH, Sur M, Lin C-S. Double representation of the body surface within cytoarchitectonic area 3b and 1 in “SI” in the owl monkey (aotus trivirgatus). J Comp Neurol 1978;181:41–73. 10.1002/cne.901810104. [PubMed: 98537]

[23]. Kaas JH, Nelson RJ, Sur M, Lin CS, Merzenich MM. Multiple representations of the body within the primary somatosensory cortex of primates. Science 1979;204:521–3. 10.1126/science.107591. [PubMed: 107591]

[24]. Nelson RJ, Sur M, Felleman DJ, Kaas JH. Representations of the body surface in postcentral parietal cortex of Macaca fascicularis. J Comp Neurol 1980;192: 611–43. 10.1002/cne.901920402. [PubMed: 7419747]

[25]. Blankenburg F, Ruben J, Meyer R, Schwiemann J, Villringer A. Evidence for a rostral-to-caudal somatotopic organization in human primary somatosensory cortex with mirror-reversal in areas 3b and 1. Cerebr Cortex 2003;13:987–93. 10.1093/cercor/13.9.987.

[26]. Nelson AJ, Chen R. Digit somatotopy within cortical areas of the postcentral gyrus in humans. Cerebr Cortex 2008;18:2341–51. 10.1093/cercor/bhm257.

[27]. Roux F-E, Djidjeli I, Durand J-B. Functional architecture of the somatosensory homunculus detected by electrostimulation. J Physiol 2018;596:941–56. 10.1113/JP275243. [PubMed: 29285773]

[28]. Schweisfurth MA, Frahm J, Schweizer R. Individual fMRI maps of all phalanges and digit bases of all fingers in human primary somatosensory cortex. Front Hum Neurosci 2014;8. 10.3389/fnhum.2014.00658. [PubMed: 24478674]

[29]. Schweisfurth MA, Frahm J, Schweizer R. Individual left-hand and right-hand intra-digit representations in human primary somatosensory cortex. Eur J Neurosci 2015;42:2155–63. 10.1111/ejn.12978. [PubMed: 26061413]

[30]. O'Neill GC, Sengupta A, Asghar M, Barratt EL, Besle J, Schluppeck D, et al. A probabilistic atlas of finger dominance in the primary somatosensory cortex. Neuroimage 2020;217:116880. 10.1016/j.neuroimage.2020.116880. [PubMed: 32376303]

[31]. Gholipour T, Koubeissi MZ, Shields DC. Stereotactic electroencephalography. Clin Neurol Neurosurg 2020;189:105640. 10.1016/j.clineuro.2019.105640. [PubMed: 31865060]

[32]. Abou-Al-Shaar H, Brock AA, Kundu B, Englot DJ, Rolston JD. Increased nationwide use of stereoencephalography for intracranial epilepsy electroencephalography recordings. J Clin Neurosci 2018;53:132–4. 10.1016/j.jocn.2018.04.064. [PubMed: 29724650]

[33]. Balestrini S, Francione S, Mai R, Castana L, Casaceli G, Marino D, et al. Multimodal responses induced by cortical stimulation of the parietal lobe: a stereoelectroencephalography study. Brain 2015;138:2596–607. 10.1093/brain/awv187. [PubMed: 26129769]

[34]. Mazzola L, Royet J-P, Catenoix H, Montavont A, Isnard J, MauguiereF. Gustatory and olfactory responses to stimulation of the human insula. Ann Neurol 2017;82:360–70. 10.1002/ana.25010. [PubMed: 28796326]

[35]. Britton JW. Electrical stimulation mapping with stereo-EEG electrodes. J Clin Neurophysiol 2018;35:110–4.10.1097/WNP.0000000000000443. [PubMed: 29499018]

[36]. Young JJ, Coulehan K, Fields MC, Yoo JY, Marcuse LV, Jette N, et al. Language mapping using electrocorticography versus stereoelectroencephalography: a case series. Epilepsy Behav 2018;84:148–51. 10.1016/j.yebeh.2018.04.032. [PubMed: 29803145]

[37]. Arya R, Ervin B, Holloway T, Dudley J, Horn PS, Buroker J, et al. Electrical stimulation sensorimotor mapping with stereo-EEG. Clin Neurophysiol 2020;131:1691–701. 10.1016/j.clinph.2020.04.159. [PubMed: 32504928]

[38]. Mullin JP, Shriver M, Alomar S, Najm I, Bulacio J, Chauvel P, et al. Is SEEG safe? A systematic review and meta-analysis of stereo-electroencephalographyerelated complications. Epilepsia 2016;57:386–401. 10.1111/epi.13298. [PubMed: 26899389]

[39]. Arya R, Mangano FT, Horn PS, Holland KD, Rose DF, Glauser TA. Adverse events related to extraoperative invasive EEG monitoring with subdural grid electrodes: a systematic review and meta-analysis. Epilepsia 2013;54: 828–39. 10.1111/epi.12073. [PubMed: 23294329]

[40]. Glasser MF, Coalson TS, Robinson EC, Hacker CD, Harwell J, Yacoub E, et al. A multi-modal parcellation of human cerebral cortex. Nature 2016;536: 171–8. 10.1038/nature18933. [PubMed: 27437579]

[41]. Setsompop K, Gagoski BA, Polimeni JR, Witzel T, Wedeen VJ, Wald LL. Blipped-controlled aliasing in parallel imaging for simultaneous multislice echo planar imaging with reduced g-factor penalty. Magn Reson Med 2012;67:1210–24. 10.1002/mrm.23097. [PubMed: 21858868]

[42]. Xu J, Moeller S, Auerbach EJ, Strupp J, Smith SM, Feinberg DA, et al. Evaluation of slice accelerations using multiband echo planar imaging at 3 T. Neuroimage 2013;83:991–1001. 10.1016/j.neuroimage.2013.07.055. [PubMed: 23899722]

[43]. Glasser MF, Sotiropoulos SN, Wilson JA, Coalson TS, Fischl B, Andersson JL, et al. The minimal preprocessing pipelines for the human connectome Project. Neuroimage 2013;80:105–24.10.1016/j.neuroimage.2013.04.127. [PubMed: 23668970]

[44]. Robinson EC, Jbabdi S, Glasser MF, Andersson J, Burgess GC, Harms MP, et al. MSM: a new flexible framework for Multimodal Surface Matching. Neuroimage 2014;100:414–26. 10.1016/j.neuroimage.2014.05.069. [PubMed: 24939340]

[45]. Robinson EC, Garcia K, Glasser MF, Chen Z, Coalson TS, Makropoulos A, et al. Multimodal surface matching with higher-order smoothness constraints. Neuroimage 2018;167:453–65.10.1016/j.neuroimage.2017.10.037. [PubMed: 29100940]

[46]. Griffanti L, Salimi-Khorshidi G, Beckmann CF, Auerbach EJ, Douaud G, Sexton CE, et al. ICA-based artefact removal and accelerated fMRI acquisition for improved resting state network imaging. Neuroimage 2014;95:232–47. 10.1016/j.neuroimage.2014.03.034. [PubMed: 24657355]

[47]. Salimi-Khorshidi G, Douaud G, Beckmann CF, Glasser MF, Griffanti L, Smith SM. Automatic denoising of functional MRI data: combining independent component analysis and hierarchical fusion of classifiers. Neuroimage 2014;90:449–68. 10.1016/j.neuroimage.2013.11.046. [PubMed: 24389422]

[48]. Glasser MF, Coalson TS, Bijsterbosch JD, Harrison SJ, Harms MP, Anticevic A, et al. Using temporal ICA to selectively remove global noise while preserving global signal in functional MRI data. Neuroimage 2018;181:692–717. 10.1016/j.neuroimage.2018.04.076. [PubMed: 29753843]

[49]. Woolrich MW, Ripley BD, Brady M, Smith SM. Temporal autocorrelation in univariate linear modeling of FMRI data. Neuroimage 2001;14:1370–86. 10.1006/nimg.2001.0931. [PubMed: 11707093]

[50]. Groppe DM, Bickel S, Dykstra AR, Wang X, Mégevand P, Mercier MR, et al. iELVis: an open source MATLAB toolbox for localizing and visualizing human intracranial electrode data. J Neurosci Methods 2017;281:40–8. 10.1016/j.jneumeth.2017.01.022. [PubMed: 28192130]

[51]. Fischl B FreeSurfer. NeuroImage 2012;62:774–81. 10.1016/j.neuroimage.2012.01.021. [PubMed: 22248573]

[52]. Hamberger MJ, Williams AC, Schevon CA. Extraoperative neurostimulation mapping: results from an international survey of epilepsy surgery programs. Epilepsia 2014;55:933–9. 10.1111/epi.12644. [PubMed: 24816083]

[53]. Bouton C, Bhagat NA, Chandrasekaran S, Herrero JL, Markowitz N, Espinal E, et al. Decoding neural activity in sulcal and white matter areas of the brain to accurately predict individual finger movement and tactile stimuli of the human hand. Front Neurosci - Neuroprosth 2021:699631. 10.3389/fnins.2021.699631. In press.

[54]. Avanzini P, Abdollahi RO, Sartori I, Caruana F, Pelliccia V, Casaceli G, et al. Four-dimensional maps of the human somatosensory system. Proc Natl Acad Sci USA 2016;113:E1936–43. 10.1073/pnas.1601889113. [PubMed: 26976579]

[55]. Ray S, Crone NE, Niebur E, Franaszczuk PJ, Hsiao SS. Neural correlates of high-gamma oscillations (60–200 Hz) in Macaque local field potentials and their potential implications in electrocorticography. J Neurosci 2008;28:11526–36. 10.1523/JNEUROSCI.2848-08.2008. [PubMed: 18987189]

[56]. Ray S, Hsiao SS, Crone NE, Franaszczuk PJ, Niebur E. Effect of stimulus intensity on the spike-local field potential relationship in the secondary somatosensory cortex. J Neurosci 2008;28:7334–43. 10.1523/JNEUROSCI.1588-08.2008. [PubMed: 18632937]

[57]. Kuehn E, Haggard P, Villringer A, Pleger B, Sereno MI. Visually-driven maps in area 3b. J Neurosci 2018;38:1295–310. 10.1523/JNEUR-OSCI.0491-17.2017. [PubMed: 29301873]

[58]. Kramer DR, Kellis S, Barbaro M, Salas MA, Nune G, Liu CY, et al. Technical considerations for generating somatosensation via cortical stimulation in a closed-loop sensory/

motor brain-computer interface system in humans. J Clin Neurosci 2019;63:116–21. 10.1016/j.jocn.2019.01.027. [PubMed: 30711286]

[59]. Freeman WJ, Rogers LJ, Holmes MD, Silbergeld DL. Spatial spectral analysis of human electrocorticograms including the alpha and gamma bands. J Neurosci Methods 2000;95:111–21. 10.1016/S0165-0270(99)00160-0. [PubMed: 10752481]

[60]. Stippich C, Ochmann H, Sartor K. Somatotopic mapping of the human primary sensorimotor cortex during motor imagery and motor execution by functional magnetic resonance imaging. Neurosci Lett 2002;331:50–4. 10.1016/S0304-3940(02)00826-1. [PubMed: 12359321]

[61]. Huber L, Finn ES, Handwerker DA, Bönstrup M, Glen DR, Kashyap S, et al. Submillimeter fMRI reveals multiple topographical digit representations that form action maps in human motor cortex. Neuroimage 2020;208:116463. 10.1016/j.neuroimage.2019.116463. [PubMed: 31862526]

[62]. Winawer J, Parvizi J. Linking electrical stimulation of human primary visual cortex, size of affected cortical area, neuronal responses, and subjective experience. Neuron 2016;92:1213–9. 10.1016/j.neuron.2016.11.008. [PubMed: 27939584]

[63]. Kim SS, Gomez-Ramirez M, Thakur PH, Hsiao SS. Multimodal interactions between proprioceptive and cutaneous signals in primary somatosensory cortex. Neuron 2015;86:555–66. 10.1016/j.neuron.2015.03.020. [PubMed: 25864632]

[64]. Ritaccio AL, Brunner P, Schalk G. Electrical stimulation mapping of the brain: basic principles and emerging alternatives. J Clin Neurophysiol 2018;35: 86–97. 10.1097/WNP.0000000000000440. [PubMed: 29499015]

[65]. Herff C, Krusienski DJ, Kubben P. The potential of stereotactic-EEG for brain-computer interfaces: current progress and future directions. Front Neurosci 2020;14:123. 10.3389/fnins.2020.00123. [PubMed: 32174810]

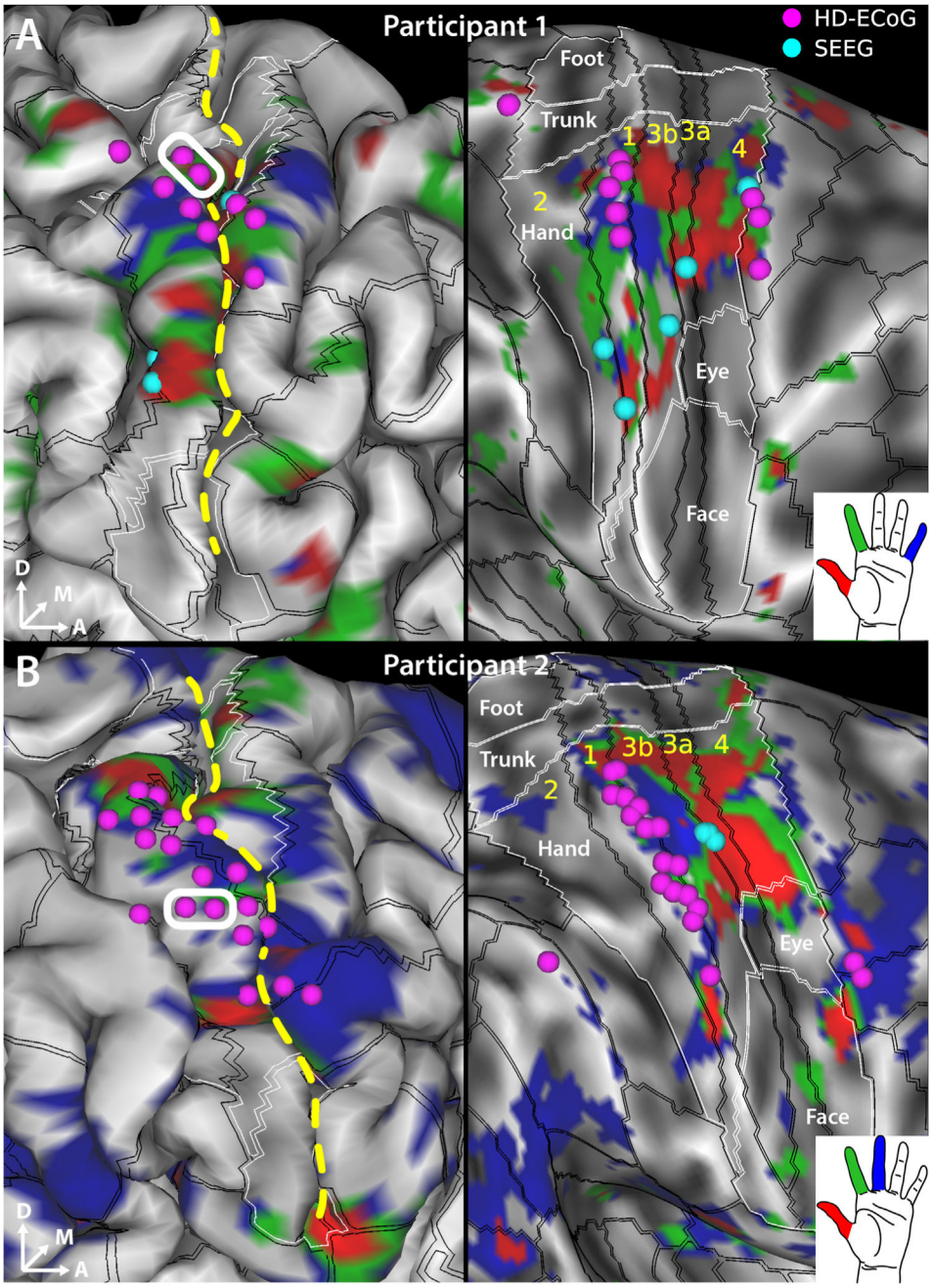

Fig. 1. fMRI activation maps for individual digits and electrode sites evoking sensory percepts in the hand region upon electrical stimulation.

Sensorimotor cortex activation map shown in **A.** for digits D1 (red), D2 (green) and D5 (blue) in participant 1 and in **B.** for digits D1 (red), D2 (green) and D3 (blue) in participant 2. SEEG (cyan spheres) and HD-ECoG (fuchsia spheres) electrodes that evoked at least one sensory percept in the hand area are overlaid over the pial surface (left panels) and over the "very-inflated" representation of the cortical surface (right panels). An example bipolar electrode for HD-ECoG is shown (white rectangle). The black lines overlaid on the cortical surface delineate the cortical areal boundaries outside of sensorimotor cortex, and

sensorimotor subregional boundaries inside sensorimotor cortex as derived from the HCP S1200 group average parcellation [40] based on myelin and cortical thickness maps and are labeled in yellow letters. The white lines demarcate the labeled somatotopic sensorimotor subregions based on resting state and task-based fMRI. The sensorimotor subareas are denoted by the intersection of the black and white boundaries. Gray shading denotes curvature of the cortical surface. Dashed yellow line denotes the central sulcus.

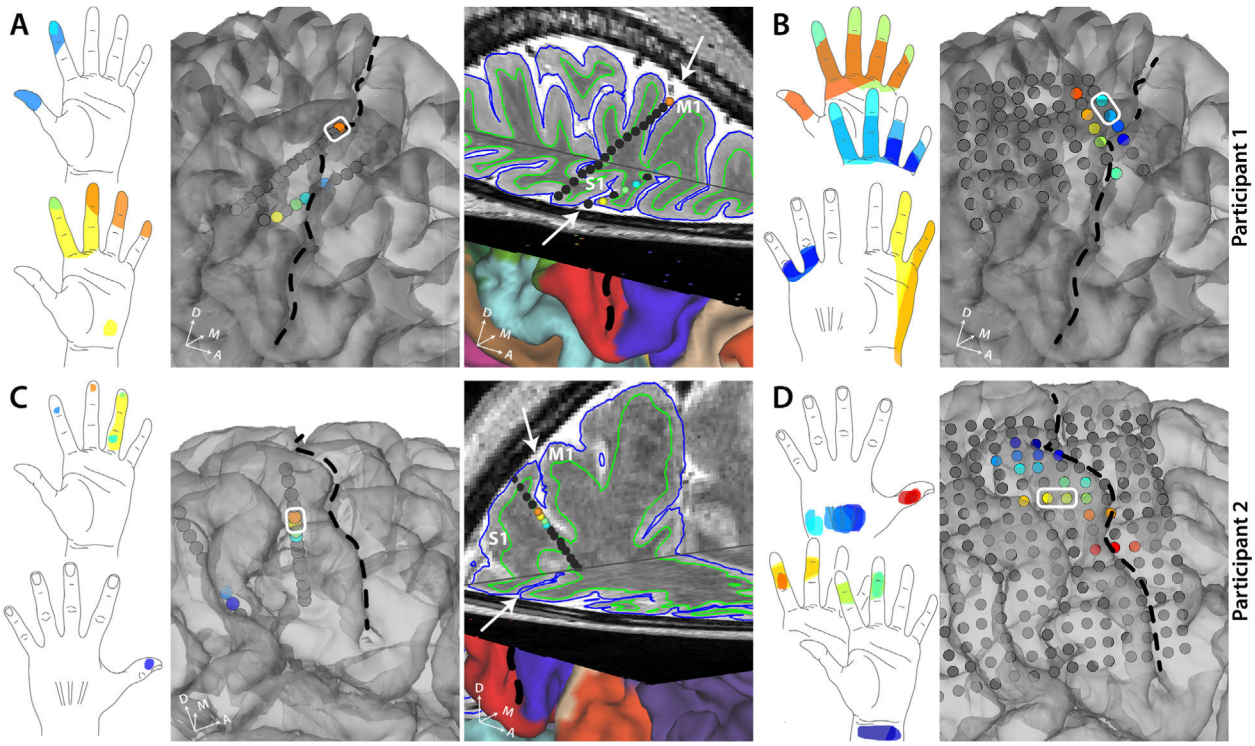

Fig. 2. Self-reported sensory percepts in the hand upon stimulation in S1 sulcal (SEEG) or gyral (HD-ECoG) areas.

A. All the sensory percepts reported by participant 1 upon sulcal stimulation through SEEG electrodes. The color of each electrode matches the color of the corresponding percept evoked. The third panel shows a 3D brain slice showing the same SEEG electrodes. **B.** All the sensory percepts reported by participant 1 upon gyral stimulation through HD-ECoG electrodes.**C.**All the sensory percepts reported by participant 2 upon sulcal stimulation through SEEG electrodes. The color of each electrode matches the color of the corresponding percept evoked. The third panel shows a 3D brain slice showing the same SEEG electrodes. Note the more posterior SEEG lead is not shown only in this panel but in Supplementary Fig. S3. **D.** All the sensory percepts reported by participant 2 upon gyral stimulation through HD-ECoG electrodes. An example bipolar electrode is shown (white rectangle). Black dashed line and white arrows denote the central sulcus.

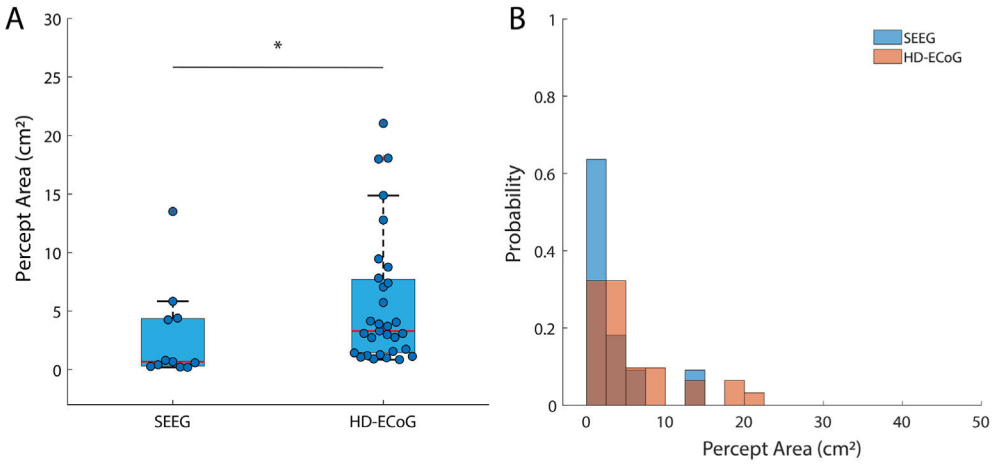

Fig. 3. Sensory percepts evoked by sulcal stimulation tend to be more focal in fingers.

A. Boxplot showing the distribution of the areas covered by sensory percepts evoked by SEEG-mediated sulcal stimulation and HD-ECoG-mediated gyral stimulation. * denotes significance in a Wilcoxon ranksum test, $\chi 2 = 5.57$; $p = 0.02$. **B.** Histograms showing frequency of occurrence of percepts of different sizes for sulcal (blue) and gyral (orange) stimulation. The two distributions are significantly different in a Kolmogorov-Smirnov test, $p \ll 0.01$.

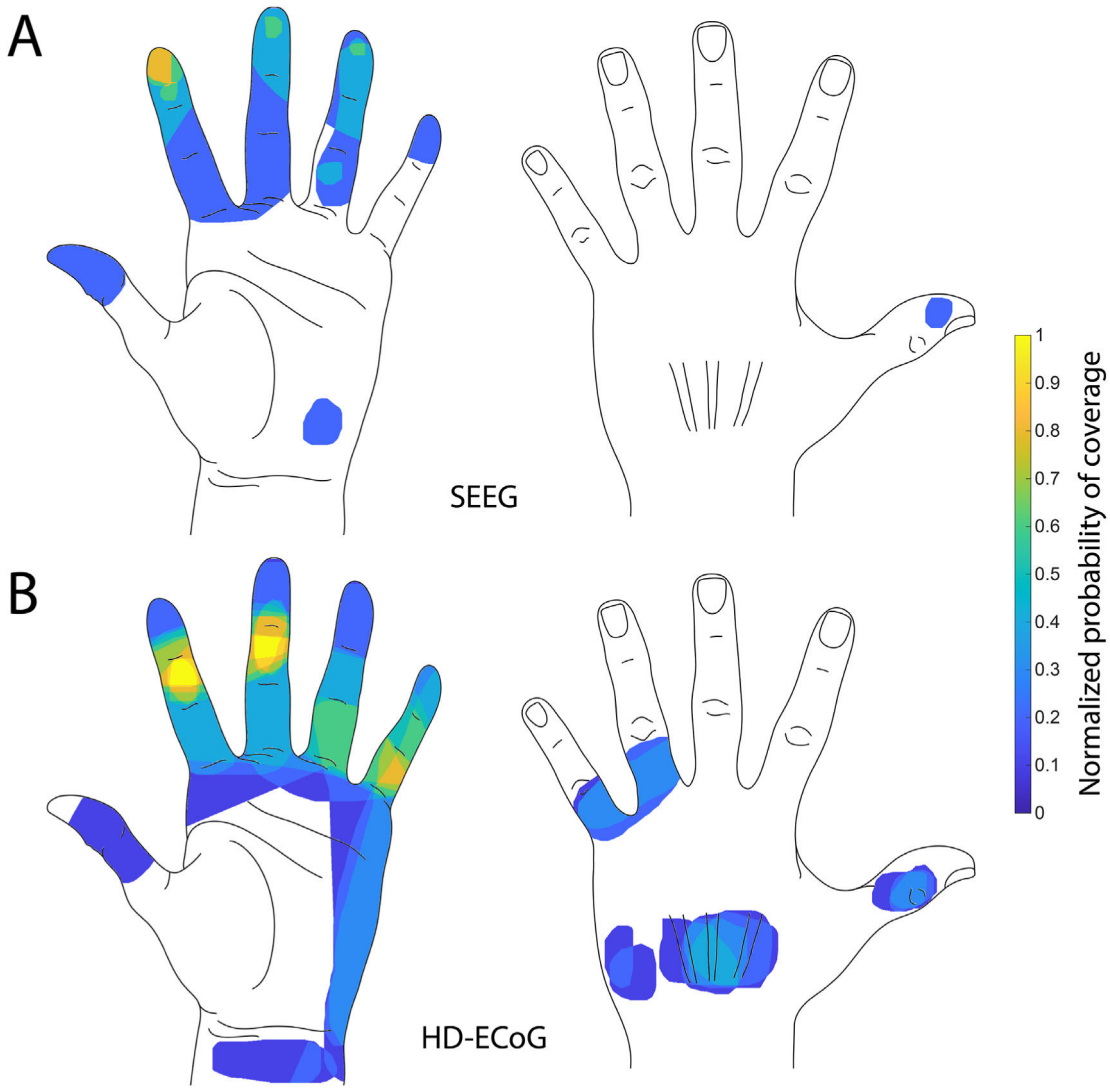

Fig. 4. Heatmap of evoked percepts.

A. Heatmap shows frequency of any region of the hand being part of a sensory percept evoked by S1 sulcal stimulation pooled from both participants. **B.** Heatmap shows frequency of any region of the hand being part of a sensory percept evoked by S1 gyral stimulation pooled from both participants. Number of percepts covering a region of the hand were normalized to the maximal number of percepts covering any area of the hand (n = 5 for SEEG; n = 10 for HD-ECoG).

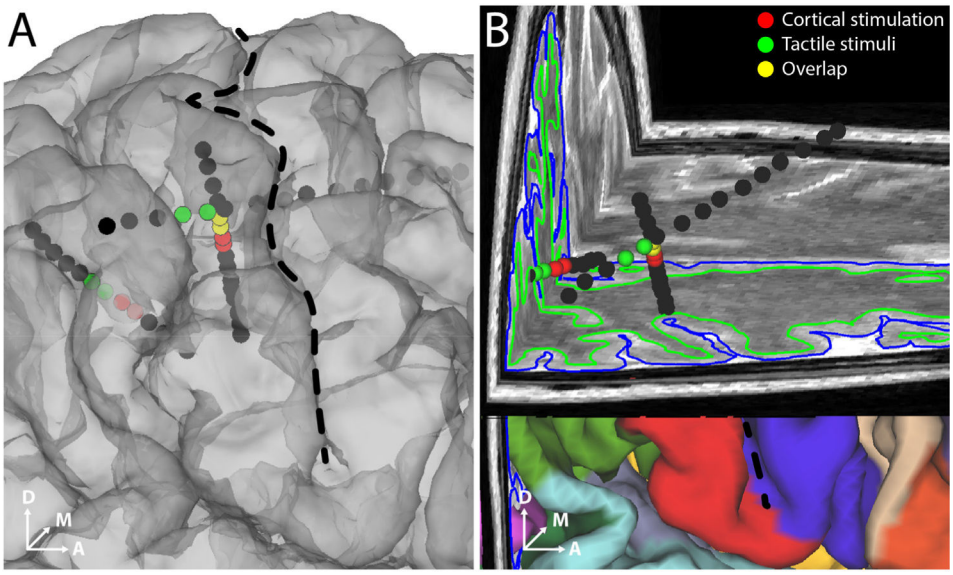

Fig. 5. Recorded neural activity correlated with tactile stimulus of fingertips in participant 2.

A and B. Electrodes that showed high degree of repeatability ($r > 0.6$) of features across mechanical tactile stimulation cycles are shown (green spheres). The electrodes that evoked a percept in the hand area are also shown (red spheres). Overlapping electrodes are shown in yellow. Black dashed line denotes the central sulcus. **B.** shows a 3D brain slice showing the same SEEG electrodes.

Table 1

Proportion of electrode that evoked sensations.

Table showing total number of electrodes that were observed to be in S1 and nearby white matter, number of electrodes that evoked a sensory percept alone and number of electrodes that evoked a sensory percept in the hand and wrist region.

Participant	Type of electrode	Total in S1	No. of electrode pairs that evoked tactile sensation alone	No. of electrode pairs that evoked sensation in hand and wrist
Participant 1	SEEG	28	17	5
	HD-ECoG	22	10	10
Participant 2	SEEG	28	6	6
	HD-ECoG	57	28	18

Table 2

Sensory percept details for participant 1.

Table provides the electrode details, stimulation parameters that evoked a sensory percept in participant 1 and the percept description. All percepts were felt only in the contralateral (left) hand.

Electrode Type	Lead/Grid	Electrode Pair	Threshold Amplitude (mA)	Frequency (Hz)	Percept Description
SEEG	RFp	7–8	0.5	20	Index and thumb
	RFp	9–10	0.5	20	Electrical sensation index fingertip
	RFp	10–11	0.8	20	Front of index and thumb
	RFp	12–13	3	50	Digits 1–2 and then palm
	RPa	1–2	0.65	20	Electrical sensation
					Digits 3–5, only tips
HD-ECoG	HDG	3–4	0.8	50	Intense tingling
					Digits 4–5 on dorsal surface
	HDG	4–5	0.72	50	Intense tingling
					Digits 4–5, on dorsal surface and down to the top of the palm just below
	HDG	5–6	0.7	50	Tingling
					Digits 2–5, center of digits (not fingertips), on dorsal surface
	HDG	6–7	1	50	Twitching sensation
					Digits 2–3, entire finger involved
	HDG	9–10	1.3	50	Tingling index finger, dorsal surface
	HDG	11–10	0.6	50	Tingling
					Digits 3–5, dorsal surface
	HDG	12–11	0.7	50	Tingling
					Digits 4–5, dorsal surface
	HDG	12–13	1	50	Tingling, pinky finger
	HDG	13–14	1.3	50	Twitching sensation in pinky
	HDG	15–14	1.77	50	Tingling in fingers

Table 3

Sensory percept details for participant 2.

Table provides the electrode details, stimulation parameters that evoked a sensory percept in participant 2 and the percept description. All percepts were felt only in the contralateral (left) hand.

Electrode Type	Lead/Grid	Electrode Pair	Threshold Amplitude (mA)	Frequency (Hz)	Percept Description
SEEG	RPs	9–10	0.5	20	Tingling
					Digit 4, towards bottom of finger
	RPs	10–11	0.5	20	Tingling
					Digit 4 fingertip; some sensation in digit 3
	RPs	11–12	0.65	20	Tingling, whole of digit 4
	RPs	12–13	1	20	Tingling, Digit 3 fingertip
	RPi	5–6	4.8	20	Tingling by the thumb
	RPi	6–7	2.1	20	Tingling index finger, small spot
HD-ECoG	HDG	39–40	1.5	50	Tingling, wrist
	HDG	40–41	1.7	50	Tingling, wrist
	HDG	54–55	1.66	50	Tingling, palm
	HDG	55–56	1.2	50	Tingling, palm
	HDG	56–57	1.8	50	Tingling, palm
	HDG	57–58	5.7	50	Tingling, palm
	HDG	71–72	5.71	50	Tingling, dorsal surface below digit 5
	HDG	72–73	0.85	50	Tingling, dorsal surface below digit 5
	HDG	85–86	1.7	50	Tingling, Digit 3, inside surface
	HDG	86–87	2.38	50	Tingling, Digit 3, inside surface
	HDG	101–102	1.8	50	Tingling, Digits 2–3
	HDG	102–103	2.1	50	Tingling, Digits 2–3
	HDG	103–104	1.2	50	Tingling, Digits 2–3
	HDG	104–105	2.08	50	Tingling, Digits 2–3
	HDG	116–117	5	50	Tingling, Digit 2
	HDG	117–118	1.95	50	Tingling, Digit 2
	HDG	147–148	1.95	50	Tingling, thumb (dorsal on knuckle)
	HDG	148–149	3.43	50	Tingling (dorsal on knuckle)

Electrode Type	Lead/Grid	Electrode Pair	Threshold Amplitude (mA)	Frequency (Hz)	Percept Description
	HDG	149–150	2.45	50	Tingling (dorsal on knuckle)